INCREASING GEOMETRIC ACCURACY OF DMC'S VIRTUAL IMAGES

M. Madani, I. Shkolnikov

Intergraph Corporation, Alabama, USA (mostafa.madani@intergraph.com)

Commission I, WG I/1

KEY WORDS: Digital Aerial Cameras, Camera Calibration, Bundle Adjustment, Self-calibration, Geometric Correction, Accuracy

ABSTRACT:

In the last two to three years, there have been a number of investigations into the geometric accuracy of large format digital cameras, particularly for large scale and engineering application. Geometric calibration of a silicon pizza image from a multi-camera platform seems to be the most challenging issue. The main problems in this effort include a combined camera lens and imaging raster frame calibration at the same time and a multi-camera platform exterior orientation (EO) calibration. Not corrected systematic image errors reduce the image accuracy and can propagate unfavorably into object space during aerial triangulation. This leads to a lower vertical accuracy of determined object points. In this paper, two different methods are used to remove or model the remaining systematic errors of the DMC (Intergraph Digital Mapping Camera) virtual images: the first method tries to remove systematic image errors by a posteriori interpolation treatment of the image residuals from bundle adjustments of test field blocks. Correction grids are then used as inputs in the DMC Post-processing software to generate virtual images or used in the real-time math model of the ImageStation products. The second method tries to describe the systematic errors using "proper" sets of additional parameters in self-calibration bundle adjustments. These methods were applied on the several DMC test blocks of varying GSDs (Ground Sampling Distances). This study showed that the magnitude of the remaining systematic errors of the image residuals is constant and ranges between 0.5µm and 3µm. Furthermore, these methods were able to increase the vertical accuracy of the object points by a factor 2 to 4 times.

1. INTRODUCTION

Intergraph's Digital Mapping Camera (DMC), introduced into the market in early 2003, is based on Charge Coupled Device (CCD) frame (matrix) sensor and provides a very high interior geometric stability. The camera was designed to perform under various light conditions with a wide range of exposure times. Features such as electronic Forward Motion Compensation (FMC) and 12-bit per pixel radiometric resolution for each of the panchromatic and color channel camera sensors provide the capabilities of operating even under less than favorable flight conditions. The DMC System allows you to produce small-scale or large-scale images with ground resolutions of fewer than two inches. The results are images with greatly improved radiometric resolution and increased accuracy of photogrammetric measurements.

The DMC itself is a digital aerial camera consisting of 8 sensors: 4 panchromatic sensors and 4 multi-spectral sensors. The multi-spectral sensors are 3k x 2k in size, with one sensor capturing red data, one capturing blue data, one capturing green data, and one capturing near-infrared data. The four panchromatic sensors each capture one image of a particular area (7k x 4k), which slightly overlap one another and are used to produce one large mosaicked image, 7680 x 13824 in size. From the image data captured by the camera, you can produce a variety of output types using the Postprocessing software.

The image data that the camera captures is stored on the Solid State Disk (SSD) which is attached to the camera system. This storage unit can easily be detached from the DMC and replaced by an empty one during the photo flight.

Figure 1. DMC with gyro stabilized mount and SSD

The DMC Postprocessing Software (PPS) is used for producing virtual images from the raw image data. Postprocessing is completed in two steps: radiometric processing and then geometric processing. Radiometric postprocessing compensates for the effects of defect pixels, the individual sensitivity of each single CCD pixel, vignetting, the influence of aperture, and the filter influence (for correction on multi-spectral images). The intermediate images, generated from the radiometric processing, are then geometrically corrected for lens distortion using the laboratory calibration parameters of the individual camera heads and are subsequently combined to form the image composite (Dörstel, 2003).

Thousands of the DMC projects have been successfully flown by different customers all over the world. All these DMC projects achieved the required accuracy standards for different photogrammetric applications established by several organizations such as ASPRS, NMAS, etc (Madani, et. al, 2004). These results have been achieved despite the smaller base-to-height ratio of the DMC by the higher image coordinate accuracy resulting from a better radiometric quality, and in particular, by better system geometry. However, some DMC users and research institutions have indicated that there is still a very small systematic error left in the DMC virtual images which leads to a lower vertical accuracy of determined object points of the large scale engineering projects.

In this study, two methods for modelling the remaining systematic errors in the so-called virtual image plane of the DMC imagery are analyzed: bundle adjustment with collocation trend refinement of the image residuals and self-calibrating bundle adjustment.

These two approaches are analyzed on several DMC test blocks having different GSDs. The ImageStation Automatic Triangulation (ISAT) software is modified to generate correction grids by collocation technique, as well as to import correction grids created by significant additional parameters of self-calibration bundle adjustment programs. The Post Correction Grid ON/OFF enabled status is controlled by the ImageStation Photogrammetric Manager “Edit Camera” dialog. Grid group and grid names can be any ANSI strings; the camera name must correspond to that in the camera file. These ISAT modifications also allow verifying the quality of these correction grids before they are used in generating new “distortion free” virtual images by DMC’s Postprocessing software (Madani, 2008).

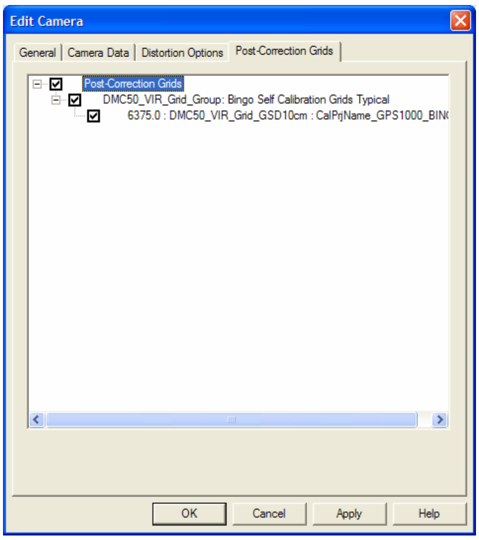

Figure 2. Edit Camera dialog

2. DMC ERROR BUDGET EVALUATION

Lens-Chip distortion of each PAN camera contains about 93% unstable “linear” (magnification, shift) part and about 7% relatively stable “nonlinear” part. Magnification (focal length change) and shift (principle point change) of each PAN camera must be fully compensated (directly or indirectly) in the platform orientation of the 4 PAN cameras. The uncompensated “nonlinear” part is the primary source of the systematic error, which directly propagates into virtual image rectification (VIR) camera space and affects platform orientation. The upper limit for the uncompensated distortion is about 2[um], which corresponds to about 8% of the total nonlinear distortion (24[um]). The estimated variation of the uncompensated nonlinear part with temperature is only 0.25[um]. So, the primary error source is a very stable constant term (Madani, 2008, Dörstel 2007).

Platform orientation, which is responsible for refinement to the relative orientation of 4 PAN cameras and compensation for the “linear” part of the lens-chip distortion, is sensitive to uncompensated nonlinear error. However, a constant systematic effect from the primary error source on platform orientation produces a constant systematic response. Error in platform orientation that propagates to VIR image space as 4-quadrant perspective distortion is the secondary error source. In total, about 35% of the systematic error in VIR space is due to primary error source and 65% is due to secondary error source.
The minimal reliable estimate of the systematic distortion present in the DMC virtual panchromatic imagery by averaging all image residuals from block adjustment within a cell-grid placed on the camera frame is about 0.5[um]. The maximal observed distortion estimate is about 3-5[um], while random image feature measurement error due to radiometric noise is 2[um].

The unknown portion of the total systematic error in image space propagates into object space, causing block shape deformation (bending, twisting, wobbling, or similar). It is contributing to an increase in discrepancy on the vertical component of the check points by 3-4 times over the undistorted values achieved by the properly calibrated cameras or bundle block adjustment of DMC photos with 4-quadrant-based self-calibration. For example, for project “Rubi” (Alamus, 2006) with GSD of 10[cm], the Z residual is about 20[cm] versus 5[cm] when the cumulative image distortion is removed. For reference, direct effect of 3[um] in image space contributes to only 0.6[cm] in object space for a single photo of this project scale; therefore, the rest of Z-distortion comes from the accumulated error causing block deformation. This deformation is visible as a “banana curve” in Z-residuals of GPS observations along a strip with the relaxed statistical weights.

3. SYSTEMATIC ERROR COMPENSATION

Traditionally, cameras are calibrated in laboratories and their systematic distortions are modelled to a considerable extent, but they always leave some kind of residual systematic errors due to their own limitations. Different camera calibration methods are used to model these residual systematic errors (Madani, 1985):

- Pre-calibration (Laboratory)
- On-the-job (Test Field) calibration (Camera intrinsic model)
- Self-calibration (Physical and Geometric models)
- A posteriori interpolation treatment of image residuals (Correction grid by Collocation)

In the following sections, only self-calibration and a posteriori interpolation techniques are briefly discussed.

3.1 Self-Calibration Method

Self-calibration is defined as the functional extension of the Collinearity equations. Different two-dimensional additional parameter (AP) models (physical, geometrical, or combinations of both) are used for expressing the unaccounted systematic distortions. However, there are certain problems with the self-calibration method:

- Treatment of additional parameters as block or photo invariants or combinations of both
- Operational problems; that is, the total strategy of assessing blunders, errors in control points, and systematic errors
- The determinability checking of APs; that is, excluding indeterminable APs from the system
- Significance testing of APs.

Each one of the above issues requires careful evaluation and proper use of the APs. The successful solution of the normal equations of the self-calibrating bundle adjustment is governed by the extent of the *correlation* between the unknown parameters (AP coefficients, exterior orientation (EO) parameters, and object coordinates). If any two parameters, for instance, are highly correlated, both tend to perform the same function. In such a case, one or the other can be suppressed without losing much information. Therefore, it is very important to study the correlation structure of unknown parameters and to check the determinability of APs.

Self-calibration APs compensate for the remaining distortion in both object space and image space of a single camera. The DMC has 4 physical PAN sensors; therefore, only a 4-quadrant self-calibration of VIR imagery may become truly effective (Kruck, 2006, Riesinger, 2006, Honkavaara, 2006, Jacobsen, 2007). However, the only purpose of such self-calibration is to "unbend" the block during triangulation. For the sake of better accuracy in object space, self-calibration may significantly overcompensate the actual distortion in image space at the frame edges. Also, it is very dependent on given object space distortions. Therefore, under no circumstances should such correction function be used in post-orientation math or applied directly to VIR production. A reason for such overcompensation is that the polynomial model has been derived to effectively compensate systematic distortions in areas concentrated around so-called Von Gruber centers or similar arrangements in camera frame format.

This approach is useful when there is no precise GPS data and no significant redundancy of image observations for sufficiently dense grid computing is available. However, due to stiffness of polynomial models, the resulting correction grid may have significant overcompensation at the edges of the image frame, which prevents the creation of a reliable ortho mosaic. When self-calibration bundle adjustment is performed for the DMC, the obtained EO can directly be used in the real-time math models of almost any softcopy system without any extra on-the-fly corrections, because the amount of image distortion itself that directly propagates into the object space is much smaller than the block bending caused by EO shift in Z. So, once good EOs are obtained, the extra correction in image space is not necessary. However, to ensure decorrelation of the obtained EO from self-calibration parameters, a compensating single photo resection on the densified triangulation (obtained in self-calibration bundle adjustment) is recommended. Once a self-calibrating bundle adjustment is performed, the obtained triangulation is densified into control and the self-calibration model itself is discarded. The following single photo resection estimates the best EO that fits the image to the ground. Unfortunately, not all photogrammetric organizations have appropriate bundle adjustment programs and technical staffs to perform such self-calibrating aerial triangulations. Furthermore, some DMC users only deliver virtual images to their customers, and they do not process or get into any photogrammetric applications. Therefore, a better and simpler procedure is needed to allow DMC owners to produce almost "distortion-free" virtual images.

3.2 Correction Grid by Collocation Method

This method does not really belong to the camera calibration methods mentioned above. In this method, some a posteriori interpolation treatment is performed on the image residuals of a bundle block adjustment. Calculated mean image residuals then serve as correction values at the interpolation points of the grid. The correction grid is able to remove the systematic errors in the image plane that could not be computed or modelled by APs in a self-calibration bundle adjustment. This correction grid application works the same way as "Reseau" to refine image coordinates for the local systematic errors by bi-linear interpolation.

4. FLIGHT SPECIFICATIONS FOR CORRECTION GRID CALIBRATION

In order to create a reliable correction grid array with collocation techniques, a highly accurate ABGPS aerial photography of about 200 to 400 images having 60% forward overlap and 80% side overlap, with ground sample distance (GSD) of 5-10, 10-20, 20-40 cm, and with a reasonable number of well-distributed ground control points are required. At a minimum, a single grid at 10cm may be computed.

A number of DMC blocks with different configurations are used for this study. General specifications of some of these blocks are given in Table 1.

DMC ID (Project Name)	**DMC 50**	**DMC 48**	**DMC 27**
Flying Height [m]	1000	800	750
GSD [cm]	10	8	7.5
% Forward Overlap	80	80	60
% Side Overlap	80	80	80
Number of Strips/Cross Strips	10/ 10	13 / 2	27 / 2
Number of Images	379	376	1105
Number of Control Points	8	21	39
Number of Check Points	6	20	14
Control Std Devs (X, Y, Z) [cm]	3, 3, 4	2, 2, 2	3, 3, 3
GPS Std Devs (X, Y, Z) [cm]	3, 3, 4	3, 3, 3	5, 5, 5

Table 1. Project specifications

The procedure to create the correction grid by Collocation techniques is as follows:

a) Perform bundle block adjustment on a block of virtual images.
b) Compute mean image residuals per square cell (about 256x256 pixels). Each image cell should have at least 40 points in order to have a reliable correction grid.
c) Compute some sort of smoothing of the trend surface with either low-pass Gaussian kernel or least square surface splines.
d) Refine image coordinates with this "Correction Grid" using bi-linear interpolation.
e) Repeat steps (a-d) 3 to 4 times until maximum residual trend increment per cell drops to lower than 0.5[um].
f) Use the correction grids in the DMC Postprocessing software to generate "distortion free" virtual images.

Repeat steps (a-d) 3 to 4 times until the maximum residual trend increment per cell drops lower than 0.5[um]. Use the correction grids in the DMC Postprocessing software to generate "distortion free" virtual images.

Alternatively, correction grids can be generated from self-calibration bundle adjustments. Exported correction grids should cover the entire virtual image format. Otherwise, image coordinates outside the correction grid must be extrapolated, which will give wrong results. These correction grids can be imported in the DMC Postprocessing software for refining virtual images, in the image observation refinement process, and in the object to image projection (real-time math model of the digital photogrammetry workstations).

5. NUMERICAL RESULTS

5.1 DMC50 Calibration and Testing

In the following sections, only results of the DMC50 block are presented. Results and conclusions of other test blocks were similar; therefore, they are not reported here.

ImageStation Automatic Triangulation is used to generate tie/pass points (Madani, 2001) for the DMC50 block. This block is then adjusted by using GPS with block shift correction (no IMU is used) and 10 microns for standard deviation of image points (tight constraints in object space and loose ones in image space force all the errors to go into the image space, where it will be captured by the collocation model). The general adjustment statistics are given in Table 2 and distributions of control/check points are given in Figure 3.

Sigma =2.9, RMS x=2.7, RMS y = 2.6 [um]	X[m]	Y[m]	Z[m]
RMS of 8 Control Points	0.017	0.029	0.019
RMS of 6 Check Points	0.020	0.032	0.047
MAX of 8 Control Points	0.035	0.043	0.030
MAX of 6 Check Points	0.036	0.049	0.067
RMS GPS	0.007	0.009	0.019
GPS Block Shift	-0.028	-0.033	0.218

Table 2. DMC50 general adjustment statistics

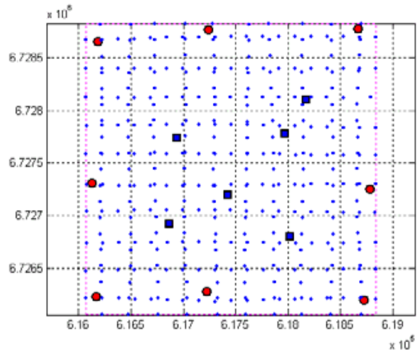

Figure 3. Distribution of control "red circles", check "blue squares", and photo centers "red circles"

5.1.1 Correction Grid generation

For a reliable estimation of the residual trend surface that is almost free from influence of clusters of small outliers, the recommended density of image residuals per 256x256-pixel cell should be between 20 to 40 points. A histogram of image points per cell and spatial distribution of cumulative redundancy number per cell (which serves as weight factor in collocation fit) are given in Figure 4.

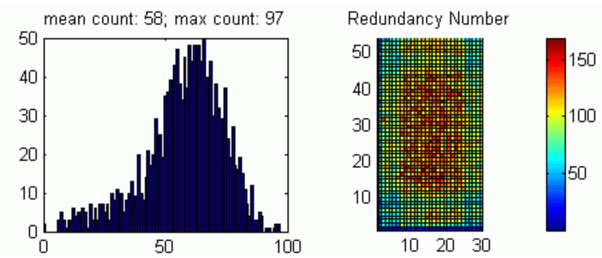

Figure 4. Histogram of image points and cumulative redundancy number distribution per cell

The collocation fit has converged to a trend surface after 4 iterations performed with the previously adjusted reference block. The estimated systematic distortion and the remaining residual trend are given in Figure 5.

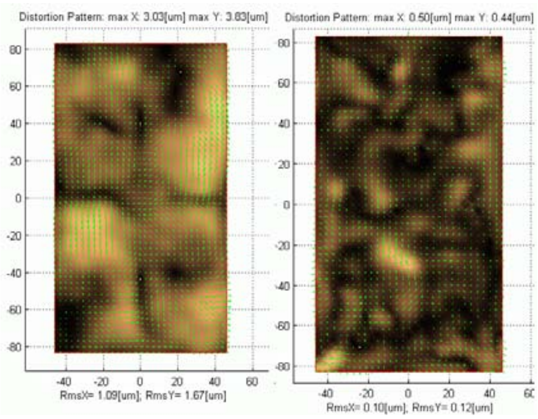

Figure 5. DMC50 VIR correction grid and the remaining distortion trend

As one can observe, the maximal estimated distortion per component (x or y) is 3.83[micron] or 0.32[pixel]. The result of the bundle adjustment of this calibration block using refined image coordinates and with standard deviation of 2 microns is given in Table 3. RMS Z values have virtually not changed after collocation fit, which is usually the case since the collocation trend simply subtracted the systematic part leaving random error virtually in the same least-squares state.

Sigma=2.5[um] RMS x = 2.4, RMS y = 2.2	X[m]	Y[m]	Z[m]
RMS of 8 control points	0.017	0.027	0.021
RMS of 6 check points	0.018	0.029	0.036
MAX of 8 control points	0.032	0.042	0.037
MAX of 6 check points	0.026	0.048	0.052
RMS GPS	0.033	0.040	0.025
GPS Block Shift	-0.029	-0.032	0.219

Table 3. DMC50 calibration block adjustment statistics

5.1.2 Post-Correction Analysis of a Test Block

The main goal of the DMC VIR correction grid is to reduce DTM block bending in Z. Generally, it cannot improve much RMS of the check points in a block with dominant local deformations. Therefore, the only reliable estimate of the improvement in DTM shape achieved after grid correction is to monitor a mean trend difference between some reference DTM shape and the test block shape, before and after correction. This particular block constitutes a situation when one cannot trust very sparse check point statistics and must rely on the mean trend estimate.

In lieu of a separate test block, a sub-block of the DMC50 project with 4 strips, 38 images, and 60% / 30% overlaps is selected. Automatic aerial triangulation is run on this selected sub-block. The reference mean DTM shape is computed from 38 images with calibration conditions (i.e., using tight GPS and loose image constraints). The uncorrected sub-block is triangulated using 8 control points only (no GPS/IMU) and tight image constraints (Std Dev = (2[um]). The mean DTM shape deformation is computed by subtracting the DTM mean surface of the uncorrected test block from that of the reference block (see Figure 6). A similar procedure is repeated with the corrected sub-block: a test block of 38 images has been reprocessed in the DMC PPS with a correction grid applied and re-triangulated following the same procedure applied to the block of uncorrected photos. The attenuation of DTM bending in this case is 3.36 times (see Figure 7).

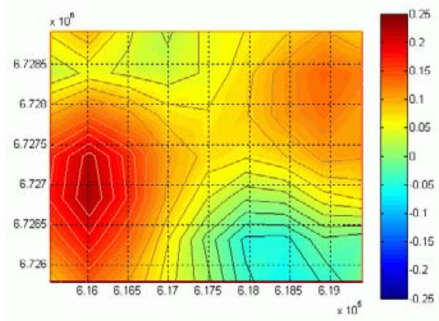

Figure 6. Block DTM bending in Z
(uncorrected block – reference block) max=0.226[m]

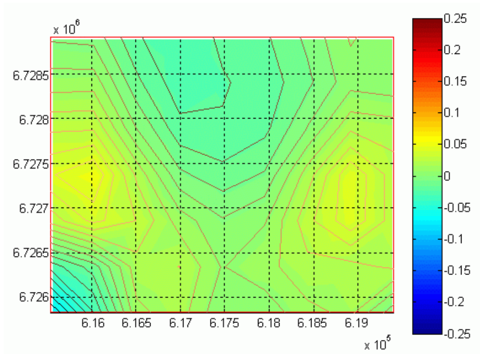

Figure 7. Block DTM bending in Z
(uncorrected block – reference block) max=0.067[m]

5.1.3 Analysis of Collocation Grid versus Self-Calibration Grid

Self-calibration bundle adjustments were also performed on the DMC50 block using different bundle adjustment programs (PATB with 44-parameter polynomials (Gruen, 1978)), BLUH with one and four sets of APS (Jacobsen, 2007), and BINGO with one and four-sets of APs (Kruck, 2006). Significant APs from these self-calibrating bundle adjustments were used to generate the correction grids. The mean trend differences between DTMs computed with collocation and self-calibration adjustments, using different bundle adjustment programs, as well as the collocation and self-calibration grids are given in Figures 8 to 12.

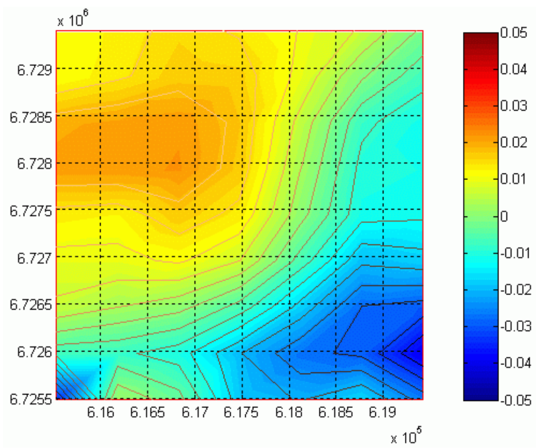

Figure 8. Mean DTM trend difference, max=0.04[m]
ISAT vs. PATB

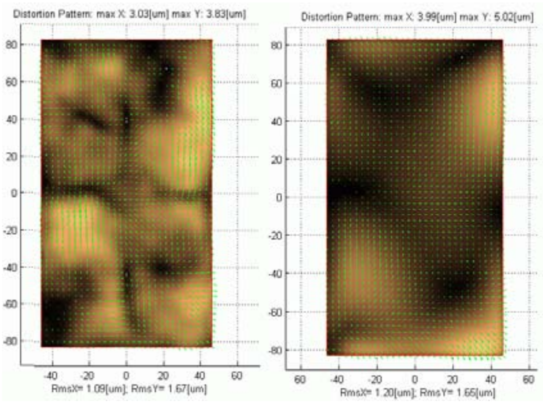

Figure 9. DMC50 collocation grid vs. PATB grid

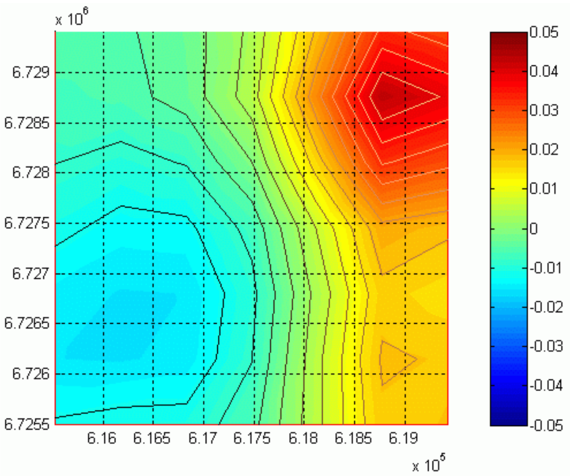

Figure 10. Mean DTM trend difference, max=0.04[m]
ISAT vs. BLUH

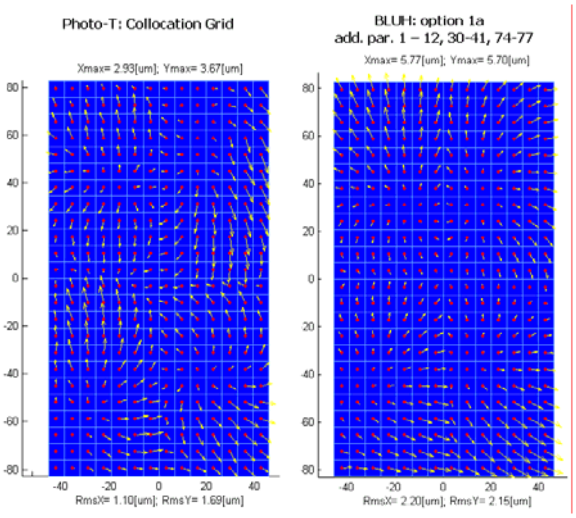

Figure 11. DMC50 collocation grid vs. BLUH grid

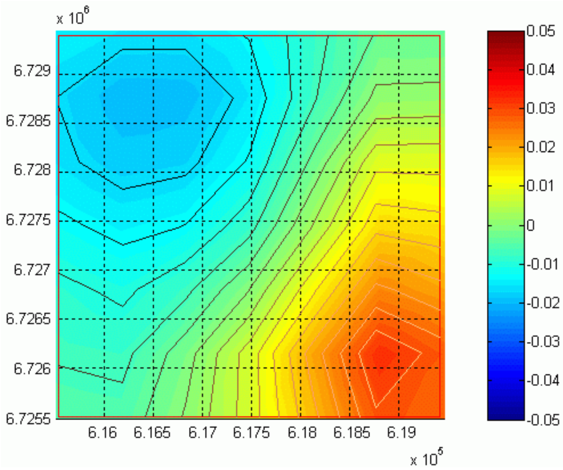

Figure 12. Mean DTM trend difference, max=0.03[m]
ISAT vs. BINGO (Typical Model)

As one can see from Figures 8-12, the maximum DTM trends in Z between ISAT collocation and three self-calibration bundle adjustment programs differ by about only 4 cm, which is within the error range on check points; thus, they have the same accuracy within precision of the method. However, the systematic grid pattern in image space that has led to almost identical block shape in object space is quite different between the methods. In total, the maximal difference between two grids (collocation and self-calibration) is equal to 5[um], which means that self-calibration overcorrects (on the edges) almost a half pixel. Since collocation grid represents true residual trend in image space, the difference between any of self-calibration grids and collocation grid is the amount of true systematic distortion left in image space after self-calibration grid refinement. So, the price to pay for correcting the block geometry in object space using self-calibration grid is to have significant systematic error in image space, possibly even larger than the initial systematic error. Such overcorrection at the edges may pose significant problems for assembly of ortho mosaics, and definitely the VIR grid correction in DMC PPS derived from self-calibration does not provide “distortion-free” images.

6. CONCLUSIONS AND FUTURE WORK

Six DMC cameras have been calibrated for VIR correction grid using the collocation method. In this paper, the DMC50 block has been used to compare several self-calibration grids to the collocation grid. Test sub-blocks of different configurations (regular 60/30 layout of 38 photos, 60/60 layout of 89 photos, and the whole calibration block of 1105 photos with 60/80 layout) have been used to measure the effect of DTM unbending by application of a VIR correction grid. The most reliable estimate of the unbending effect is the mean DTM trend difference between a GPS-constrained test block and unconstrained test block (sparse control at the edges of the block). This configuration produces the maximal block bending, and the mean DTM trend difference (and its maximum) serves as a robust estimate of the improvement in DTM shape. The robustly-computed mean trend is free from the effects of local deformation affecting sparsely distributed check points. The total attenuation of DTM bending on a sub-block selected from the calibration block ranges 2-4 times. The expected attenuation for any other block (flown at a different GSD) is about 2 times due to the large project-dependent part of the systematic error. It is very important in the future to measure DTM bending on a block flown at a different GSD than the one used to produce a single correction grid. In case such effect is significantly reduced, an array of correction grids needs to be computed to cover the span of all probable GSDs.

The main recommendation delivered in this work is that, given a photogrammetric block with sufficient redundancy of image observations and precise given EO, the best approach to obtain a correction grid is to perform a bundle adjustment with collocation. When precise GPS is available, the GPS-derived Direct Geo Referencing (DGR) EO is used. When no precise GPS is available, the self-calibrating bundle adjustment is preformed to obtain precise EO and densified control points. The DMC virtual images should be generated using the correction grids during DMC Postprocessing.

Another direction of future work is to capture the systematic distortion in the individual four PAN cameras by a collocation grid using a calibration flight with proper overlap of PAN camera footprints (i.e., all parallel strips flown in one direction). This work will take care of 35% of total DMC error. Another effort is to refine the geometric platform calibration procedure to significantly reduce the remaining 65% of DMC error by utilizing strong correlation of platform orientation parameters from exposure to exposure along a strip.

REFERENCES

Alamús, R., Kornus W., Talaya, J. (2006): Studies on DMC Geometry. ISPRS Journal of Photogrammetry & Remote Sensing, Vol. 60, pp 375-386.

Dörstel C., 2007. DMC - (R)evolution on geometric accuracy, in: Fritsch D. (Ed.), Photogrammetric Week 2007, Wichmann, Heidelberg.

Dörstel C., 2003. DMC - Practical experiences and Photogrammetric System Performance, in: Fritsch D. (Ed.), Photogrammetric Week 2003, Wichmann, Heidelberg.

Grün, A. (1978): Progress in Photogrammetric Point Determination by Compensation of Systematic Errors and Detection of Gross Errors. International Society for Photogrammetry, Symposium of Commission III, Moscow, USSR.

Honkavaara, E., et. al. (2006): Complete Photogrammetric System calibration and Evaluation in the Sjökulla test field – Case Study with the DMC. In: EuroCow 2006 Proceedings Barcelona.

Jacobsen, K. (2007): Geometry and Information Contents of Large Size Digital Frame Cameras, ASPRS Annual Conference, Tampa, Florida, May 7-11, 2007.

Kruck, E. (2006): Simultaneous Calibration of Digital Aerial Survey Cameras. In: EuroCow 2006 Proceedings Barcelona.

Madani, M., Shkolnikov, I. (2008): International Calibration and Orientation Workshop, January 30th – February 1st, 2008, Castelldefels, Spain.

Madani, M., Dörstel C., Heipke C., Jacobsen K. (2004): DMC practical experience and accuracy assessment. In: ISPRS Proceedings 2004 Istanbul.

Madani, M (2001). Z/I Imaging New Automatic Aerial Triangulation System, ASPRS Annual Conference, St. Louis, MO, April 23-27, 2001.

Madani M., (1985). Accuracy Potential of Non-Metric Cameras in Close-Range Photogrammetry Ph.D. Dissertation, Department of Geodetic Science and Surveying, The Ohio State University.

Riesinger, I (2006): Investigations on DMC (Digital Mapping Camera) Auto-Calibration, Diploma Thesis, Munich Technical University, Germany, 2006.